Photoreactive Anatase Consolidation Characterized by FTIR Spectroscopy

Jeffrey R. S. Brownson, M. Isabel Tejedor-Tejedor, and Marc A. Anderson*

Environmental Chemistry and Technology Program, University of Wisconsin−Madison, 660 N. Park Street, Madison, Wisconsin 53706

Received July 18, 2005. Revised Manuscript Received October 3, 2005

Titania (anatase) thin films were consolidated and hardened via UV irradiation when acidic precursor sols were diluted with 1-, 2-, and 3-carbon aliphatic alcohols. Titania sols were adjusted to pH values of 1.4, 2.3, or 3.1 and subsequently diluted with various mole fractions (X_{ROH}) of alcohol prior to film deposition. Re-esterification of the titania film surface was confirmed by transmission FTIR (Fourier transform infrared) spectroscopic characterization. In the dark (absence of UV), proton-catalyzed oxidation of the alkoxide functional groups produced a unique monodentate formic acid ligand. This further oxidized to bidentate bicarbonate and carbonate complexes. Given an equivalent fluence of UV light (20 J cm^{-2}, 254 nm), films became harder with increased proton concentration and X_{ROH}. UV light promoted formic acid and carbonate/bicarbonate removal by photocatalytic oxidation. The rate of loss of formic acid/bicarbonate species following UV irradiation increased with increasing proton concentration. With respect to carbon chain length, film hardness was found to follow MeOH > EtOH > ^{n}PrOH for pH 1.4 and X_{ROH} = 0.48.

Introduction

Among the many applications for titania, including use as a photocatalytic oxidant of pollutants and as a film for self-cleaning glass, it also serves as an essential component in photovoltaics.[1−6] The effects of sol preparation techniques on particle coarsening, surface area loss, and surface chemistry modification in titania films are significant for the next generation solar cells, the dye-sensitized "Grätzel cell", and inorganic "*eta*-cell" that can use nanoparticulate TiO_2 for charge transfer.[6,7] Maintaining a high surface area is particularly important in this case, as the significant portion of the material reacting to the absorption of light is the interfacial monolayer of dye or inorganic "*e*xtra-*t*hin *a*bsorber" film. Lower temperature processing helps to maintain higher surface areas in these films. Dye-sensitized cells have been produced on flexible substrates such as poly(ethylene terephthalate) (PET), generating interest in processing titania films at lower temperatures relative to conventional thermal sintering techniques.[8−11]

Recently, we reported the existence of a low-temperature method of hardening anatase films using supra-band gap UV light in the presence of humidity.[12] The addition of a 0.48 mole fraction of ethanol to the initial sol was found to re-esterify the titania surface with ethoxide functional groups and to produce carboxylate oxidation products. However, several researchers have indicated that methanol acts as an even more favorable esterification reactant on titania surfaces.[13,14] The methanol to methoxy surface functionalization was found to be thermodynamically "barrierless" for anatase.[13] As such, studies of the changes in surface chemistry that occur during the addition of primary alcohols and during the hardening process under UV irradiance are valuable.

Experimental Procedures

Film Synthesis. Nanoparticulate suspensions of TiO_2 (sols) used in this study were synthesized as described previously.[12,15] Briefly, anatase titania sols were adjusted to three initial values of pH with nitric acid (1.4, 2.3, and 3.1) and each diluted with ethanol or methanol to achieve mole fractions of alcohol: X_{ROH} = 0.33, 0.40, 0.48, and 0.57 for comparison. To maintain the solids concentration for each alcohol (8 g/L total solid content), a balancing mole fraction of water of the desired pH was added. The alcohols lowered the surface tension of the suspension for spray deposition, promoting the quick drying of the film, and also changed the solvent

* To whom correspondence should be addressed. Tel.: 608-262-2674. Fax: 608-262-0454. E-mail: nanopor@wisc.edu.

(1) Bahnemann, D. W.; Mönig, J.; Chapman, R. *J. Phys. Chem.* **1987**, *91* (14), 3782.
(2) Hoffmann, M. R.; Martin, S. T.; Choi, W.; Bahnemann, D. W. *Chem. Rev.* **1995**, *95*, 69.
(3) Wang, R.; Hashimoto, K.; Fujishima, A.; Chikuni, M.; Kojima, E.; Kitamura, A.; Shimohigoshi, M.; Watanabe, T. *Nature* **1997**, *388* (6641), 431.
(4) Kormann, C.; Bahnemann, D. W.; Hoffmann, M. R. *J. Phys. Chem.* **1998**, *92*, 5196.
(5) Nosaka, Y.; Kishimoto, M.; Nishino, J. *J. Phys. Chem. B* **1998**, *102*, 10279.
(6) O'Regan, B.; Grätzel, M. *Nature* **1991**, *353*, 737.
(7) Könenkamp, R.; Dloczik, L.; Ernst, K.; Olesch, C. *Physica E* **2002**, *14*, 219.
(8) Pichot, F.; Pitts, J. R.; Gregg, B. A. *Langmuir* **2000**, *16*, 5626.
(9) Lindström, H.; Holmberg, A.; Magnusson, E.; Lindquist, S.-E.; Malmqvist, L.; Hagfeldt, A. *Nano Lett.* **2001**, *1* (2), 97.
(10) Oekermann, T.; Zhang, D.; Yoshida, T.; Minoura, H. *J. Phys. Chem. B* **2004**, *108*, 2227.
(11) Miyasaka, T.; Kijitori, Y. *J. Electrochem. Soc.* **2004**, *151* (11), A1767.
(12) Brownson, J. R. S.; Lee, T. J.; Anderson, M. A. *Chem. Mater.* **2005**, *17* (11), 3025.
(13) Wang, C.; Groenzin, H.; Schulz, M. J. *J. Phys. Chem. B* **2004**, *108*, 265.
(14) Kim, K. S.; Barteau, M. A.; Farneth, W. E. *Langmuir* **1988**, *4*, 533.

10.1021/cm051568f CCC: $30.25
Published on Web 11/04/2005

environment of the titania particles. A secondary dilution experiment was prepared using ^{n}PrOH to test the hypothesis that carbon chain length influences the film hardness ($X_{nPrOH} = 0.48$, pH 1.4). Inorganic films ($X_{ROH} = 0$) of each pH were prepared and tested for the absence of organics on the surface using FTIR spectroscopy (as described below). Then the inorganic films were dipped into 0.05 M formic acid solutions adjusted to three values of pH (1.4, 2.3, and 3.1). The films were left to soak for 2 h, then dried, and characterized again by FTIR spectroscopy. To compare our results of hardness tests using UV exposure with those of thermal film-processing techniques, films ($X_{MeOH} = 0.57$, pH 2.3) were deposited and fired at 150, 250, and 350 °C for 30 min, with a 30 min ramp to the set temperature. Results were compared to the larger data sets of MeOH and EtOH dilutions.

Coating was performed using a novel low-pressure WideTrack ultrasonic spray system, also described previously.[12] Films were deposited using 3.0 W applied to the 60 kHz horn, with a 15 mL/min sol delivery rate and a conveyor line speed of 5 ft/min. The system delivered uniform coatings on both glass slides and Si wafers that gelled quickly with thicknesses between 150 and 300 nm as determined by ellipsometry. All glass replicates and the Si wafer used for testing were passed through the path of the spray simultaneously. Fluid lines (PFA tubing) were purged with 20 mL of the diluting solvent prior to and following spraying to eliminate cross-contamination of alcohols. Our previous study found humidity to be a relevant parameter in film hardening and surface hydrolysis of alkoxides.[12] Therefore, all films were dried and stored under vacuum at room temperature immediately after deposition to minimize hydrolysis reactions of the surface organics and used within 2 days of coating.

Photoreactor Design. A reactor for controlled temperature and relative humidity (RH) was constructed in line with a high irradiance monochromatic light source. The main reactor box was UV-opaque poly(methyl methacrylate) (PMMA) (28.32 L/1 ft^3) with side gas ports for humidity control. A 500 W Oriel Hg(Xe) arc lamp was used as the light source. Source light was first passed through a water-cooled infrared filter and then on through a Czerny-Turner style monochromator (with 3 mm slit widths on both sides). The reactor was humidified to 40% relative humidity (RH) at 40 °C). Internal silicone-coated heat tape and a 2.5 W fan created a well-mixed environment within the reactor. The box was fitted with a 50 mm fused silica window (UV transparent) to allow the high-energy light to pass.

UV Exposure. For all experiments, a 20 J cm^{-2} fluence was employed in the photoreaction. This was determined to create sufficient hardening such that differences in tested parameters were observable and also kept films below a maximum pencil hardness of 9H, a constraint of our testing method. Experiments were performed at 40 °C and 40% relative humidity. Films were placed in the reactor and allowed to equilibrate at reactor temperature and relative humidity for 10 min before being exposed to UV light. The exposed spot size was approximately 1 cm × 0.5 cm. The 254 nm wavelength (4.88 eV) was specifically selected from our previous study for two reasons: (1) the short exposure time required to obtain the desired fluence at this wavelength (46.5 min given 7.1 mW cm^{-2} irradiance and 97% absorbance efficiency at 254 nm[12]) and (2) this wavelength is the peak irradiance of a UVB germicidal Hg fluorescent bulb, a readily available light source.

Characterization of UV Films. FTIR data were collected with a Nicolet Magna 750 spectrometer in transmission mode. The spectrometer used an MCT-A (HgCdTe) detector with KBr beam splitter (single beam, 150 scans, 1 cm^{-1} resolution, 4000−900 cm^{-1} collection window). Si wafers were used as IR-transparent substrates. Due to the high surface area per mass, mesoporous films greatly enhance the surface signal for spectral analyses, such that these spectra approximate a surface-sensitive technique. All Si wafers were placed inside a cell with a BaF_2 window (perpendicular to IR beam). The cell was flushed with zero-air for initial background collection. Following the spray deposition of the TiO_2 sol and vacuum-drying, the films were immediately transferred to the IR cell and flushed with zero-air for 1 h and 30 min. Dry spectra were then collected for films prior to UV exposure. The wafers were subsequently transferred into the UV reactor for a 20 J cm^{-2} exposure and then carefully replaced in the IR cell to be dried for 1 h and 30 min before a final post-UV spectral collection. All spectra were processed for interferometric noise reduction, background subtraction, and peak deconvolution using RazorTools/8 Bayesian data analysis programs via the Grams/AI software package. Spectra between 1800 and 900 cm^{-1} were all normalized to a consistent sharp band at 1582 cm^{-1} (assigned to a bidentate carbonate $\nu C{=}O_{II}$ stretching mode) unless mentioned otherwise in the figures. This band changed minimally in all photocatalytic oxidation experiments and reflected partitioning with respect to pH between bicarbonate species.

Hardness tests were performed on glass supports following the UV exposures. The films were subjected to pencil scratch tests by using 9H-9B Derwent Graphic pencils (Acco UK Ltd.). The pencil test follows ASTM standard procedure #D3363 for testing relative film hardness. Beginning with the hardest pencil (9H), the pencil is held at 45° and pushed away from the tester in a 1 cm stroke on a flat surface. If the pencil gouges and scribes the film, the next softer pencil is used, on down to the pencil that does not scribe the film. This is termed the pencil hardness and is a measure of the structural integrity of the film as a whole. This result is a collective measure of the film adhesion to the glass substrate as well as the interparticle connections. Tests were replicated four times for each condition to establish a confident film hardness value.

Results

The full IR spectra (4000−900 cm^{-1}) of representative thin films for methanol and ethanol systems are presented in the Figure 1A and 1B insets. The main spectral features appear between 3800 and 2600 cm^{-1} and 1800−900 cm^{-1}. All spectra displayed a very broad band from 3600 to 2900 cm^{-1}, well-known to be associated with the stretching vibrations of hydrogen-bonded surface water molecules and hydroxyl groups.[16,17] The broad width of this band indicated significant hydration of the surface. Several weak and significantly narrower peaks were convolved with the broad water region. In the main portion of Figure 1 these peaks were investigated by treating the broad water band as background. The spectra for both alcohol systems display two distinct bands at 3730 and 3667 cm^{-1}, which were assigned to stretching modes of non-hydrogen-bonded anatase surface −OH groups.[18] These two bands decreased with increasing proton concentration and with UV exposure. In addition to these peaks, a single band at 3190 cm^{-1} was tentatively assigned to the νOH of a formic acid species hydrogen-bonded to a surface oxygen.[19]

(15) Xu, Q. Ph.D. Thesis, University of Wisconsin−Madison, Madison, WI, 1991.
(16) Burgos, M.; Langlet, M. *Thin Solid Films* **1999**, *349*, 19.
(17) Kataoka, S.; Tejedor-Tejedor, I. M.; Coronado, J. M.; Anderson, M. A. *J. Photochem. Photobiol.* **2004**, *163* (3), 323.
(18) Primet, M.; Pichat, P.; Mathieu, M.-V. *J. Phys. Chem.* **1971**, *75*, 5(9), 1216.
(19) Maréchal, Y. *J. Chem. Phys.* **1987**, *87* (11), 6344.

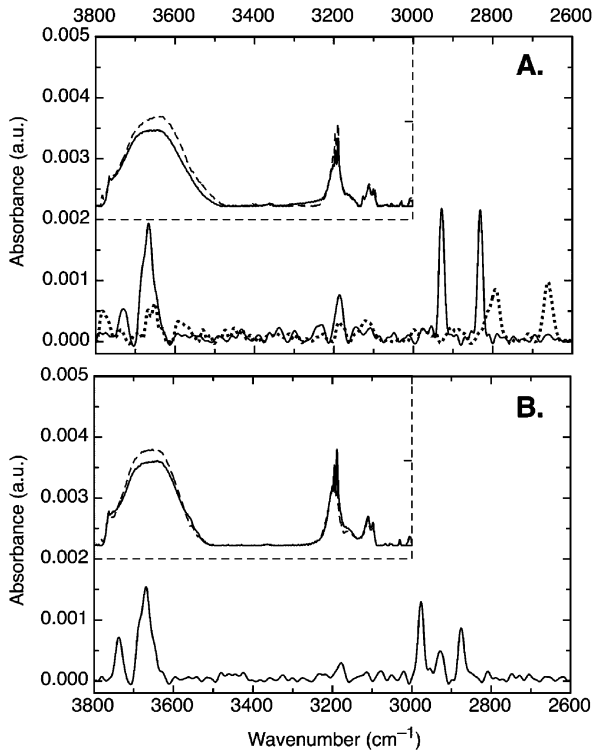

Figure 1. IR spectra from 3800 to 2600 cm^{-1} for methanol-diluted films (A): pH 3.1 pre-UV film shows methyl stretching bands (solid line) and pH 1.4 post-UV film shows formaldehyde Fermi resonance bands (dashed line). IR spectra for ethanol-diluted film (B): pH 3.1 pre-UV film displays methylene and methyl stretching bands. Inset: 3800−900 cm^{-1} spectra for pH 3.1 films for (A) and (B) before (solid lines) and after (dashed lines) UV exposure (inset: abs. unit = 2.5*x* major unit of main figures). Both spectra indicate a change in the hydrated state following UV exposure.

For Figure 1A the spectrum of the methanol system at pH 3.1 displayed two weak but distinct peaks at 2928 and 2831 cm^{-1} that were assigned to the asymmetric and symmetric methyl stretching modes of surface methoxy species, respectively. These bands have been reported also by Wang et al.[13] (by surface-specific sum frequency generation IR) and by Wu et al.[20] (by transmission IR) for methoxy species on anatase. The methyl stretching modes were observed as very weak bands in the spectrum of the pH 2.3 film (not shown) and were absent from the spectrum of the pH 1.4 film (not shown). These bands were absent in all films following UV exposure. In Figure 1A, we observed two weak peaks at 2794 and 2661 cm^{-1} following irradiation of the pH 1.4 system. These bands are very characteristic of unsaturated aldehydes and result from a Fermi resonance between νCH and the δCH overtone.[21] The presence of these two peaks confirms the formation of formaldehyde during the photocatalytic process. Formaldehyde is a highly volatile species typically found as a gas-phase product of alcohol oxidation.[16,22]

In the ethanol system, peaks at 2980, 2940, and 2880 cm^{-1} were assigned to the characteristic symmetric and asymmetric stretching modes of $-CH_2-$ and $-CH_3$ species in the surface alkoxide (Figure 1B).[16] The intensity of these bands also decreased with increasing initial proton concentrations in the sols (not shown). Ultraviolet exposure eliminated these methylene and methyl peaks from detection in all of the ethanol systems that were studied.

In Figure 2, we show IR spectra of MeOH and EtOH films before and after UV exposure for 1800−900 cm^{-1}. Bands at ∼1605 and ∼1295 cm^{-1} were assigned to the independent νC═O and νC−O modes of a highly asymmetric formic acid species. The $\Delta\nu$ for the carboxylate bands broadened with increasing proton concentration in the films. The alcohol used in synthesis did not significantly affect the position of the bands.

Figure 3 shows the region between 1750 and 1150 cm^{-1} for the pre-UV MeOH-derived film (pH 1.4, $X_{MeOH} = 0.48$, solid spectrum in upper left of Figure 2) after deconvolution, revealing characteristic bands for two carbonate species as well. A shoulder at 1630 cm^{-1} was assigned to the bending mode of water. Comparing Figures 2 and 3, bands at ∼1582 and ∼1230 cm^{-1} along with a weak band at ∼1006 cm^{-1} are proposed to be assigned to νCO_{II}, $\nu CO_I + \delta O_I CO_{II}$, and νCO_I modes of a bidentate carbonate (CO_3^{2-}) surface species, respectively. These bands were in agreement with studies reporting bidentate carbonate surface formation.[23−27] Deconvolved bands at ∼1562 cm^{-1}, a broad band between ∼1500 and 1480 cm^{-1}, and ∼1245 cm^{-1} were each assigned to the ν_aCO, ν_sCO, and δOH···O modes of a bidentate bicarbonate (HCO_3^-) species, respectively.[24,25] There was an increase in the intensity of formic acid and bicarbonate bands as the proton concentration increased. These bands also became more intense as X_{ROH} was increased (spectra not shown). Also, in each of the alcohol-diluted films, the bands associated with the formic acid and HCO_3^- complexes decreased significantly more than those belonging to the CO_3^{2-} species following UV exposure.

The alkoxide νC−O band was present in the spectra of both methanol and ethanol systems. Again in Figure 2, the methanol spectrum displayed a methoxide band at 1137 cm^{-1}, particularly for pH 3.1. This observation agrees closely with previous studies of methoxide formation by esterification from adsorbed methanol.[20] The spectrum of the ethanol system for pH 3.1 displayed bands at 1132, 1109, 1072, and 1041 cm^{-1}. These were assigned to methyl rocking modes of ρCH_3 and $\rho' CH_3$ as well as ethoxy stretching modes of νC−O and νC−C, respectively.[21] The positions of these peaks were consistent with those reported by both Burgos and Langlet[16] and Wu et al.[20] regarding ethanol adsorption and esterification to ethoxide on anatase surfaces. Specifically, the band at 1072 cm^{-1} is unique to the νC−O of ethoxide species.[16] The alkoxide stretching band decreased in intensity with increasing proton concentrations of the sols. The band was absent in the spectra of UV irradiated samples. Its removal was determined to coincide with the methylene and methyl stretching bands.

(20) Wu, W.; Chuang, C.; Lin, J. *J. Phys. Chem. B* **2000**, *104*, 8719.
(21) Roeges, N. P. G. *A Guide to the Complete Interpretation of Infrared Spectra of Organic Structures*; John Wiley & Sons: New York, 1994.
(22) Chen, J.; Ollis, D. F.; Rulkens, W. H.; Bruning, H. *Wat. Res.* **1999**, *33* (3), 661.
(23) Yates, D. J. C. *J. Phys. Chem.* **1961**, *65*, 746.
(24) Morterra, C.; Chiorino, A.; Boccuzzi, F. *Z. Phys. Chem.* **1981**, *124*, 211.
(25) Busca, G.; Lorenzelli, V. *Mater. Chem.* **1982**, *7*, 89.
(26) Liao, L.-F.; Lien, C.-F.; Shieh, D.-L.; Chen, M.-T.; Lin, J.-L. *J. Phys. Chem. B* **2002**, *106*, 11240.
(27) Nakamoto, K. *Infrared and Raman Spectra of Inorganic and Coordination Compounds−5th Ed.*; John Wiley & Sons: New York, 1997.

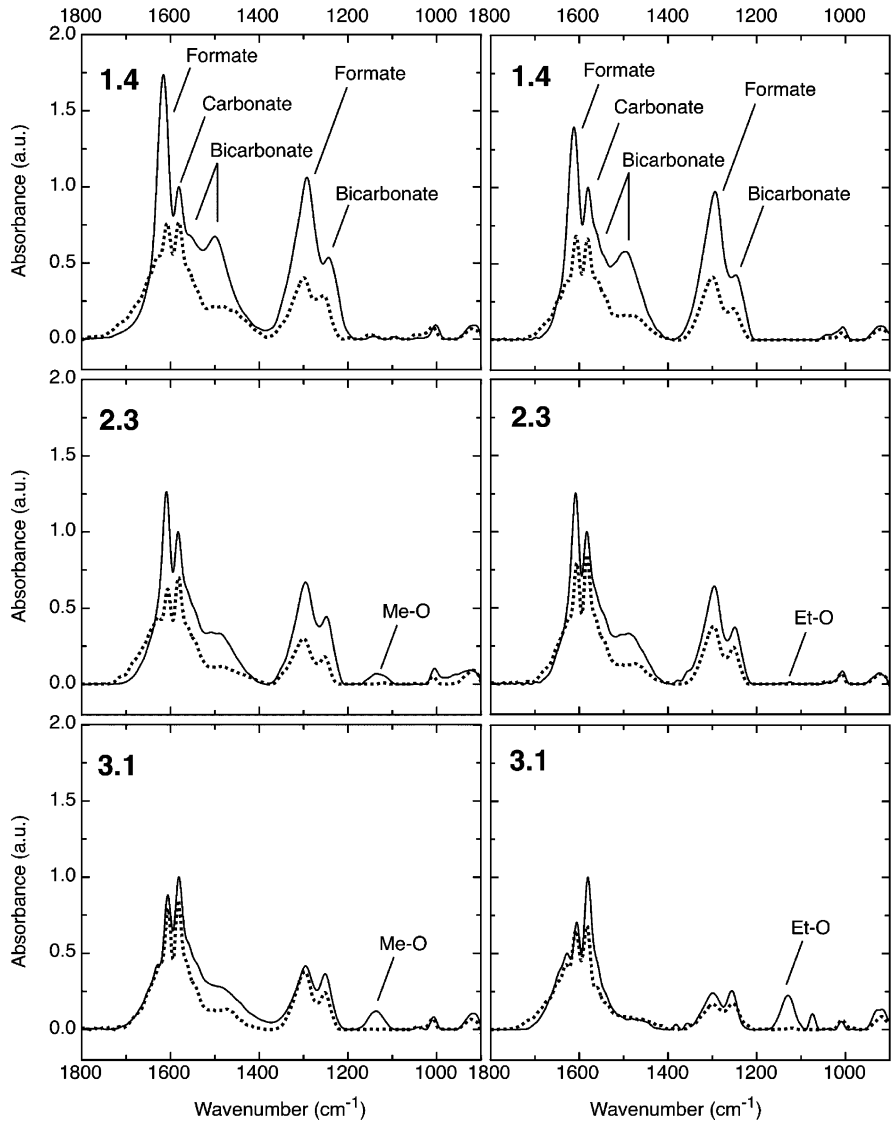

Figure 2. IR spectra of (left) MeOH dilution and (right) EtOH dilution from 1800 to 900 cm^{-1} for experiments prior to UV (solid dark line) and post-UV treatment (dashed gray line); pH of initial sol = 1.4, 2.3, 3.1.

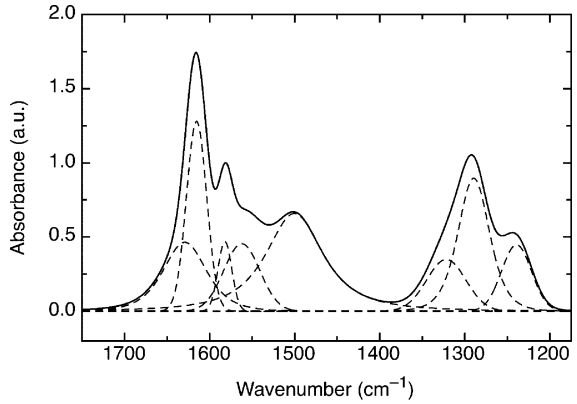

Figure 3. IR spectrum of carbonate/formate bands of MeOH film for pH = 1.4 of initial sol (solid line) and deconvolved peaks (dashed lines). Peaks were fitted using Pearson VII peak shapes in the RazorTools/8 package.

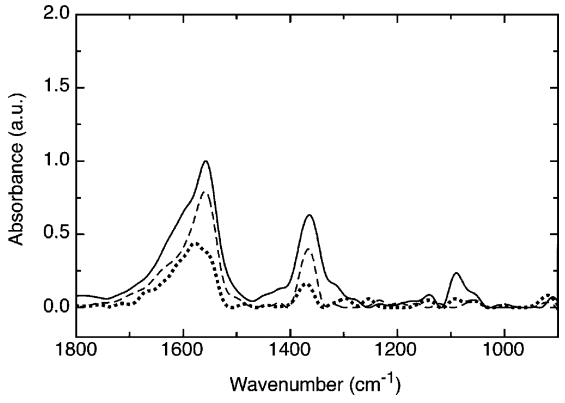

Figure 4. IR spectra of inorganic anatase film dipped into 0.05 M formate solutions adjusted to pH 3.1 (solid), 2.3 (dashed gray), and 1.4 (dotted). Spectra normalized to maximum intensity peak for a pH 3.1 film.

The experiments using purely aqueous sols to form inorganic anatase films ($X_{ROH} = 0$) were also characterized. These films showed only trace amounts of organics on the surfaces by FTIR investigation (not shown). No hardening was observed in any of the inorganic control films. After the surface chemistry was confirmed using FTIR, the inorganic films were dipped into 0.05 M formic acid solutions at pH 1.4, 2.3, and 3.1 and dried for further spectroscopic characterization. In Figure 4, we show that the resulting bands showed formate adsorption, but the $\Delta\nu$ (the wavenumber separation) of the carboxylate bands were much smaller (<200 cm^{-1}) than those observed for the alcohol

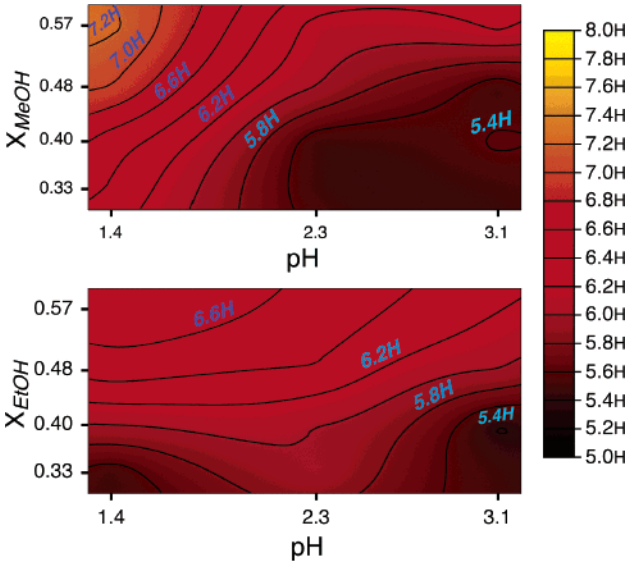

Figure 5. Film iso-hardness contours for (top) methanol dilutions and (bottom) ethanol dilutions. Curves range from pencil hardness 5H to 8H.

systems (~300−325 cm^{-1}) due to lower wavenumber band observed at ~1558 cm^{-1} and higher wavenumber band observed at ~1365 cm^{-1}. These bands were assigned to the ν_aCOO and ν_sCOO modes of a bridging bidentate formate complex in agreement with the literature.[27] There was no evidence of peaks associated with bicarbonate or carbonate complexes in these spectra.

Typical film hardness prior to UV exposure for all films was between 4 and 5H. As shown in Figure 5, film hardness following UV exposure increased with a corresponding decrease in the initial pH of the sol. This initial pH reflects the concentration of protons within the pores for the dried films. As proton concentration increased, the films increased in hardness given the same fluence of UV light. Hardness was also a function of the mole fraction of alcohol in each dilution. As the mole fraction of alcohol was increased, there was a corresponding increase in film hardness. Methanol-derived films showed a maximum hardness for both systems at pH 1.4 and for alcohol mole fractions >0.57; however, the visual quality of the films was better for films prepared from pH 2.3 sols. Films prepared for comparison with thermal processing (X_{MeOH} = 0.57, pH 2.3) were found to harden to 5H, 6H, and 7H for 30 min exposures at 150, 250, and 350 °C, respectively. Films exposed to the single wavelength of light (254 nm, 20 J/cm^2 fluence, 40 °C, 40% RH) under the same preparation conditions were found to harden slightly greater than 6H.

The film from *n*-propanol (X_{ROH} = 0.48, pH 1.4) revealed similar IR spectra as was found for methanol and ethanol under the same parameter conditions. In Figure 6 we show strong bands attributed to formic acid and bicarbonate species. Although the earlier studies with MeOH and EtOH films suggested that the ^{n}PrOH film would react well to photoreactive consolidation given a high alcohol mole fraction and proton concentration, its hardness changed minimally from 5H to 6H after UV exposure. Therefore, it appears that, at high mole fractions of alcohol and high proton concentrations, photoreactive film consolidation improved with smaller alcohol chain length.

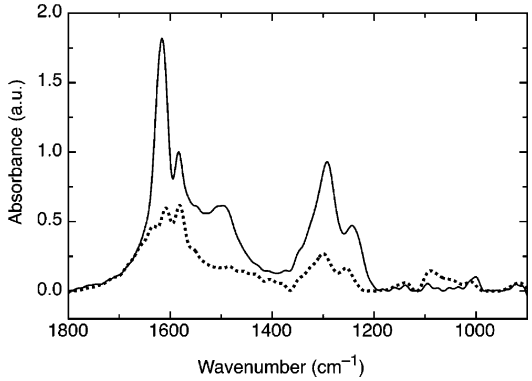

Figure 6. IR spectra of ^{n}PrOH prior to UV treatment (solid dark line) and post-UV treatment (dashed gray line).

Discussion

Speciation of Surface Organics. The wavenumber separation of symmetric and asymmetric −COO stretching bands for carboxylate species (termed $\Delta\nu$) is very diagnostic of the organic bonding environment, relative to the aqueous ionic formate ($\Delta\nu$ = 201 cm^{-1}). Monodentate complexes exhibit $\Delta\nu$ values much larger than ionic complexes. Bidentate/chelating complexes show $\Delta\nu$ values much less than the ionic species. Bridging bidentate complexes display $\Delta\nu$ values greater than chelating complexes, but near to the ionic value.[27]

Our infrared findings for the organic surface species following re-esterification suggest a uniquely adsorbed formic species, different from that of an ion or acid adsorbed from solution. The absorption bands for this species are quite distinct from those of a formate ion complex or a protonated formic acid hydrogen-bonded to the anatase surface. The combination of the observed large $\Delta\nu$ values and the unusual shifts in frequency for −COO stretching bands from expected values have led us to this interpretation.

The $\Delta\nu$ for the HCOOH species of Figures 2 and 6 are significantly greater than that of the ionic formate (347 vs 201 cm^{-1}), suggesting that a monodentate formate/formic acid species is present in these films before UV exposure. However, the unusual frequencies of the carboxylic stretching modes indicate the formation of an asymmetric bidentate complex.[27] The frequency of the band associated with the stronger −COO (1615 cm^{-1}) is very similar to the analogous stretching modes of reported monodentate formates in the literature (1604−1630 cm^{-1}). But the frequency for the longer, weaker −COO bond is rather low when compared with reported values (1289 vs 1314−1376 cm^{-1}).[25,27] Vittadini et al. have performed first principles density functional calculations for adsorbed formic acid and formate on dry and hydrated anatase (101) surfaces. They found the most stable monodentate conformation to be a formic acid ligand bound to a 5-fold coordinated Ti atom via the carbonyl group, and hydrogen-bonded to a surface oxygen via the −OH group. Vittadini et al. call this type of complex a molecular monodentate, in which no deprotonation (dissociation) occurs upon binding the surface of anatase via the carbonyl group.[28] However, it can also be regarded as essentially a bidentate

(28) Vittadini, A.; Selloni, A.; Rotzinger, F. P.; Grätzel, M. *J. Phys. Chem. B* **2000**, *104*, 1300.

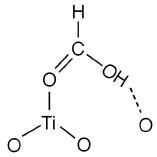

Figure 7. Schematic of proposed conformation of formic acid ligand on anatase.

formate with two very different acceptor atoms (5-fold coordinated Ti and 2-fold coordinated O) and therefore as an asymmetric bidentate. An asymmetric complex as such suggests that the stretching modes will be essentially decoupled; hence, the stretching bands have been interpreted as νC═O and νC−O in this case. This type of ligated formic acid species has been reported before in Cu/CuO systems. In the Cu/CuO adsorption studies, the authors also reported unusually low νC═O and νC−O bands and attributed the bands to a carbonyl bound to a reduced Cu site.[29,30] Given the first principles calculations of Vittadini et al. and our IR data, we propose the formation of a molecular monodentate formic acid species coordinated to the Ti through the carbonyl group and hydrogen-bonded to a surface oxygen through the hydroxyl proton (Figure 7).

The formic acid species is considered to have formed directly on the surface from the oxidation of an alkoxide precursor. Because of this direct synthesis on the anatase surface, this formic acid species may be considered to be representative of reactions on a "dry" anatase surface, as was predicted by Vittadini et al. We present this as the first confirmed incidence of the unique formic acid species found in situ, directly related to the initial covalent binding of the alkoxide species on the anatase surface from the re-esterification process. The FTIR characterization of films that were dipped into 0.05 M formate solutions for each of our tested pH values reflect dissociative adsorption of formate species. We found significantly smaller $\Delta\nu$ values than for our alcohol systems, in agreement with a bridging bidentate configuration predicted by Vittadini et al. for adsorption of formate on a hydrated surface.[28]

We also propose bicarbonate and carbonate complexes on the anatase surface prior to UV exposure. Several studies in the literature have observed IR bands for carbonate species forming due to CO_2 adsorption on the anatase surface.[23−26] The positions of the deconvoluted bands as reported in Table 1 are in close agreement with those found for bidentate bicarbonate and bidentate carbonate species. The presence of a carbonate species is not completely unexpected, as we expect a carbonate to be an intermediate species to CO_2 generation in a complete mineralization of the surface-bound organic species. The bands associated with the carbonate/bicarbonate species result from oxidation of the monodentate formate to a bidentate bicarbonate species. Given the changes in protonation states of the films, it is reasonable to propose that a partitioning between carbonate and bicarbonate would occur. For proton dissociation, bicarbonate species are favored at low pH, and the relative increase in bicarbonate with increasing proton concentration in the films reflects this finding. Given hydroxyl radical formation during UV exposure due to photocatalysis, carbonate species should be readily mineralized to CO_2.

Table 1. Assigned IR Modes and Vibrational Frequencies (cm^{-1}) for the Observed Experiments

CH_3O		C_2H_5O		water	
ν_aCH_3	2928	ν_aCH_3	2980		
		ν_aCH_2	2940		
ν_sCH_3	2831	ν_sCH_3	2880		
		ρCH_3	1132	δH_2O	1630
		$\rho'CH_3$	1109		
		νC−C	1072		
νC−O	1137	νC−O	1041		

formic acid (HCOOH)		carbonate (CO_3^{2-})		bicarbonate (HCO_3^-)	
νOH	3190				
νC═O	1615.5				
		νCO_{II}	1582.2	ν_aCO	1562.4
				ν_sCO	1500.4
		$\nu CO_I + \delta O_ICO_{II}$	1321.8		
νC−O	1289.5			δOH···O	1239.3
		νCO_I	1010		

Effect of Oxidation of Surface Organics. In Figure 2 we see that following UV irradiation for films from all alcohols, the bands associated with the bicarbonate complexes were preferentially removed from the surface during the process of photocatalysis. This removal was most evident for films derived from pH 1.4 sols in both systems. Alkoxide bands were readily oxidized and removed from the films as well, and methylene and methyl stretching bands in the 3800−2600 cm^{-1} region were interpreted as belonging to the alkoxide species. These bands were simultaneously removed via proton-catalyzed oxidation (non-UV) and photocatalytic oxidation.

As mentioned previously, absorption bands associated with non-hydrogen-bonded hydroxyl surface groups decrease in intensity with increasing proton concentration in the dried films and with UV exposure, for both MeOH and EtOH systems. Figure 2 shows that when the proton concentration in the films is increased, the intensity of the peaks attributed to the carboxylic acid and carbonate species is also increased. These results can be attributed to a decrease in the total free −OH surface density. Here, the reduced non-hydrogen-bonded hydroxyl surface density can be attributed to an increase in the rate of re-esterification with increased proton concentration. These data suggest that alkoxide ligands are eliminated by proton-catalyzed (dark) oxidation to carboxylic acids and carbonates. However, as the films are exposed to UV light, photocatalytic oxidation completes the oxidation process by mineralizing the organic byproducts to CO_2. In this way, a fresh anatase surface is exposed with very high excess free surface energy due to increased surface stress from bond distortion, allowing the TiO_2 to form interparticle bonds. For nanoparticles with extremely high surface area/volume ratios such as ours, this excess surface energy is quite high (on the order of 100−700 J g^{-1}) and interparticle bond formation is expected to be extremely favorable.[12]

Relationship between Surface Species and Hardening. Some trends in film consolidation can be clearly established from the pencil hardness data. For example, film hardening

(29) Millar, G. J.; Rochester, C. H.; Waugh, K. C. *J. Chem. Soc., Faraday Trans.* **1991**, *87* (9), 1491.
(30) Millar, G. J.; Newton, D.; Bowmaker, G. A.; Cooney, R. A. *Appl. Spectrosc.* **1994**, *48* (7), 827.

from alcohol dilutions can be observed to be a function of both the initial pH of the sol and the mole fraction of alcohol, with increasing hardening found at lower pH values (higher proton concentrations) and higher mole fractions of alcohol. However, the carbon chain length of the precursor alcohol also appears to contribute to the consolidation process. Given the reports in the literature of favorable molecular adsorption on anatase surfaces for smaller chain alcohols,[13,14] we can infer that the MeOH system exhibited a much more extensive proton-catalyzed oxidation of all alkoxide and formate species. Oxidation is proposed to proceed from methoxide to formaldehyde → formic acid → bicarbonate and then to CO_2. In comparison, we interpret the EtOH and ^{n}PrOH systems as being limited 2-fold: first, through reduced initial alcohol adsorption, and second, through a reduced efficiency of oxidation because of the need to cleave C−C bonds.[20] This is presumed to minimize the consolidation process, which depends on formic acid elimination via mineralization to CO_2.

We have found the degree of film consolidation for alcohols to follow MeOH > EtOH > ^{n}PrOH for $X_{ROH} = 0.48$ and pH 1.4. This follows the same trend as for alcohol photocatalytic oxidation efficiency, and alkoxide and carboxylic acid thermal decomposition.[22,26] Given the smallest carbon chain length, MeOH-derived films with high proton concentrations and a high alcohol mole fraction maximize initial alcohol surface coverage and provide the simplest pathway for CO_2 generation. From these data and past literature, the primary elements affecting photoreactive anatase film consolidation are presented in Table 2. Fundamentally, an organic molecule bound to the surface needs to be present that can then be mineralized to CO_2. This loss exposes a fresh titania surface with extremely high excess free surface energy, favoring interparticle bonding. The consolidation process is also aided by extremely high capillary compressive forces from interstitial pore water (on the order of 80−100 MPa), bringing the particles into close contact.[12] Hence, we propose that particles are joined in a cold welding process, combining clean surfaces via compressive pressures.

Table 2. Assignment of Dependencies in Photoreactive Hardening

1. alcohol surface saturation (SS)	$\propto^{-1}$	carbon chain length (CC)
2. alkoxide concentration (AC)	$\propto$	SS,
	$\propto$	proton concentration (PC),
3. photocatalytic oxidation (PCO)	$\propto^{-1}$	CC,
	$\propto$	PC,
	and $\propto$	relative humidity
4. formic acid concentration*	$\propto$	AC,
	$\propto$	PC,
	and $\propto$	PCO,
	(*and in the presence of an ethoxide $\propto$	C−C bond concentration)
5. bicarbonate/carbonate removal	$\propto$	formic acid concentration,
	$\propto$	AC,
	$\propto$	PC,
	and $\propto$	PCO

By comparing the film hardness for TiO_2 processing via photoreactive consolidation with that of thermal processing, we have confirmed that this novel method has potential as a low-temperature alternative for film consolidation. Due to the photocatalytic properties of anatase, films can be generated with similar hardness properties at significantly lower temperatures and shorter exposure. This study was confined to a single wavelength exposure at one low temperature (254 nm, 40 °C) and represents only partial mineralization of the surface organics. In fact, hardening via photoreactive consolidation can be improved significantly (shorter exposures, harder films) by using a broad band of UV light and temperatures higher than those applied in this study (data not shown). Organics are completely mineralized, leaving a clean, durable film for new applications with anatase.

Acknowledgment. The authors sincerely thank Cardinal CG Co. (Eden Prairie, MN) for their financial support and positive discussions regarding this research.

CM051568F